Amorphous and nanograins in the bonding zone of explosive cladding

Y. YANG*, B. WANG, J. XIONG
School of Materials Science and Engineering, Central South University, Changsha 410083, Hunan, People's Republic of China
E-mail: yangyang@mail.csu.edu.cn

Published online: 12 April 2006

The amorphous and nanograins in the bonding zone of the titanium/titanium explosive cladding were investigated by means of transmission electron microscopy (TEM) and high-resolution transmission electron microscopy (HRTEM). The nanograins with perfect crystal structure range from 2 to 50 nm in diameter were in coherent with the matrix. While the amorphous were in the state of the long-range disorder and coexisted with the nanograins. The formation of the amorphous and the nanograins as well as their coexisting were due to the high cooling rate (range from 3.55×10^6 to 7.8×10^6 K/s at the amorphous transition temperature) within the bonding zone, and the high pressure as well as the high shear stress during the explosive cladding.

1. Introduction

Amorphous was characterized by topological disordering of atoms in three dimensions and with no grain boundary and stacking fault in its microstructure. What's more, arrange of atoms in amorphous didn't like those in ideal gas that were completely disorder. In order to distinguish the amorphous and nanograin, the short-range ordered area of amorphous should less than 1.5 nanometers (nm) [1]. The preparation methods of amorphous were usual divided into two modes. The first one was extremely rapid solidification at high temperature, such as fast cooling of metal [2], sputtering [3] and so on. The second one was prepared at the room temperature or a little higher by a certain method, such as mechanical alloying, solid-state reaction amorphous [4]. Recently, some special materials, such as semiconductor phases (Si, Ge, Sb, Bi) and semiconductor compound, could be amorphous by the pressure-quenching technique quenched at liquid nitrogen temperature under certain pressure. It was named as the third mode [5].

The bonding zone in the explosive cladding was a transition area of the components, structures and performances of the base metals and had high strength. Generally, it was considered that the high strength bond was caused by the amorphous and nanograins in the bonding zone [6]. Although the width of the diffusion layer in the bonding zone was only several hundreds nm, diffusion reactions were occurred during the explosive cladding of different kinds of metals, for example, the FeTi, TiC and Fe_5C_2 etc. were existed in the diffusion layer of the titanium/mild steel explosive cladding [7]. In order to neglect the effect of the diffusion reaction, the titanium/titanium (Ti/Ti) explosive cladding was chosen. The objectives of this paper were to report observations of the amorphous and nanograins within the bonding zone and to discuss the formation reasons of amorphous and nanograins as well as the coexisting area.

2. Experimental

The annealed commercial purity titanium [TA2(α-Ti)] was used in the present work. Its grain size was ~40 μm. The α-Ti/α-Ti composite plate was achieved by constant stand-off explosive cladding technique which was described elsewhere [8]. The detonation velocity of the selected explosive was approximately 2400 m/s and the density of the explosive was 0.95–1.1 g/cm^3 and the flyer plate was about 608 m/s. Specimens for TEM and HRTEM analyses were cut from the central portion of the sheets in a plane parallel to the jetting direction and normal to the plane of the cladding interface. TEM observations were carried out in a Hitachi H-800 analytical operated at 200 kV; and HRTEM observations were performed with JEOL 2010 TEM operated at 800 kV.

*Author to whom all correspondence should be addressed.
0022-2461
DOI: 10.1007/s10853-005-5677-2

3. Results

Fig. 1 showed the microstructure in the α-Ti/α-Ti explosive bonding zone. The titanium on both sides of the interface was mainly composed of twins. While, the bonding zone was made up of lots of amorphous marked by "A" and nanograins marked by "UG".

Fig. 2 showed the pattern of nanograins in the bonding zone. It could be seen that the sizes of nanograins were range from several nm to 50 nm in diameter and distributed non-homogeneously.

Fig. 3 showed the characteristics of nanograin with the diameter only several nm. The fringes of crystal lattice image were orderly and symmetrically and the grains with perfect crystal structure were in coherent with the crystal plane $(11\bar{2}2)$ of the matrix. The fringe spacing of grain "A" in three dimensions were 1.6940Å, 1.2479Å, and 1.1189Å, respectively. They were close to the interplanar distances of $(10\bar{1}2)$,$(11\bar{2}2)$, and $(20\bar{2}2)$ in the α-Ti, which were 1.7241Å, 1.2455Å, and 1.1189Å, respectively. From above analysis, the indices of crystallographic plate were standardized, as shown in Fig. 3. Grain boundaries marked by "GB" were characterized by coherent, shown in Fig. 3. The angles between the fringe directions of the grain "A" and the matrix were 42 and 103°, respectively, shown in Fig. 4. It was concluded that the crystal structure was still close-packed hexagonal (H.C.P.) structure and the titanium in this area maintained α phase and the grain boundaries were coherent and the coherent grain boundaries guaranteed the high strength of grain boundaries.

Hammerschmidt [9] pointed out that, with the subsequent extreme rapid cooling, the newly formed nanograins within the center of the bonding zone were equiaxed grains and had rather random distribution of orientations. Therefore, the nanograins within the bonding zone should be the result of fast cooling.

Fig. 5 showed the crystal lattice image of the selected area within the bonding zone. The fringe images of many regions in the Fig. 5a were nonexistence, e.g. "G" area (in Fig. 5b). Therefore, amorphous was located in "G" area. Although fringes in "A" areas in Fig. 5a were distinct, the scales of the short-range ordered area were less than 1.5 nm, therefore, they should be considered as amorphous. The scales of the short-range ordered area within

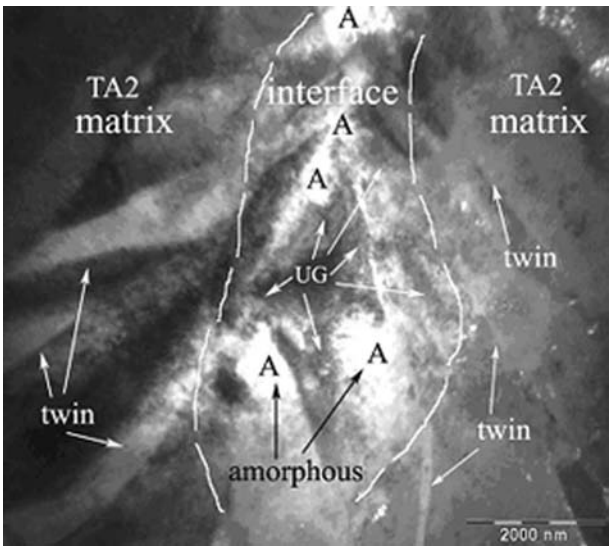

Figure 1 Microstructure in the Ti/Ti explosive bonding zone.

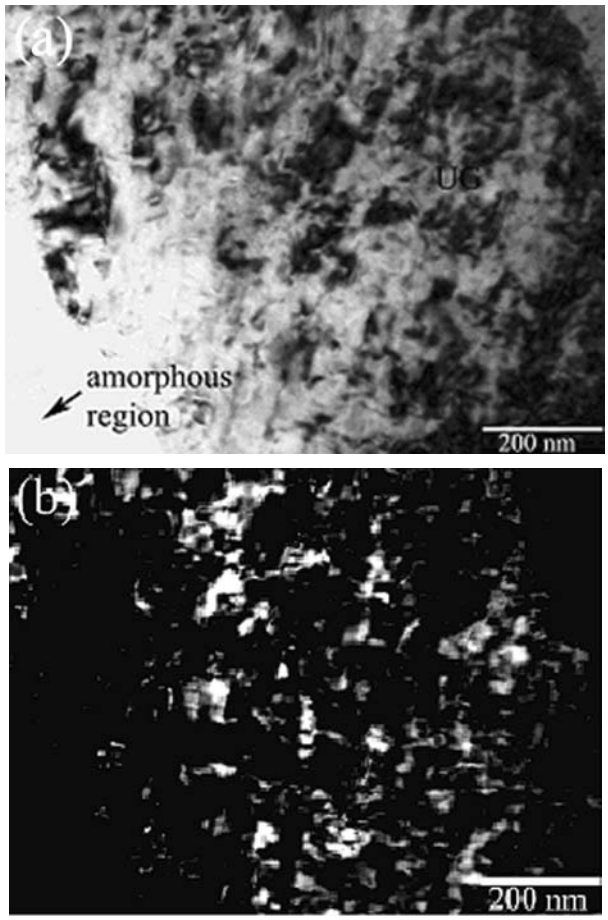

Figure 2 Nanograins in the Ti/Ti explosive bonding zone. (a) bright field image; (b) corresponding dark field image.

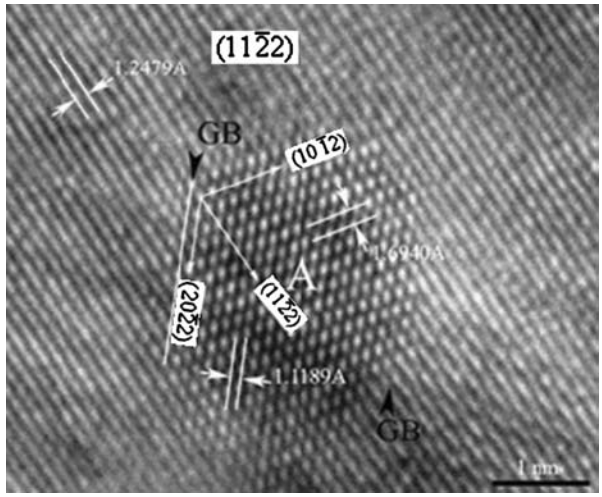

Figure 3 High-resolution crystal lattice image of nanograin in the Ti/Ti explosive bonding zone.

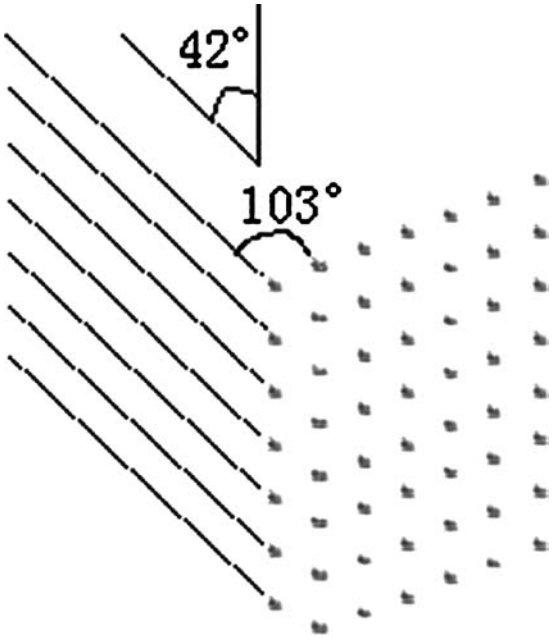

Figure 4 Schematic plan of coherent grain boundary.

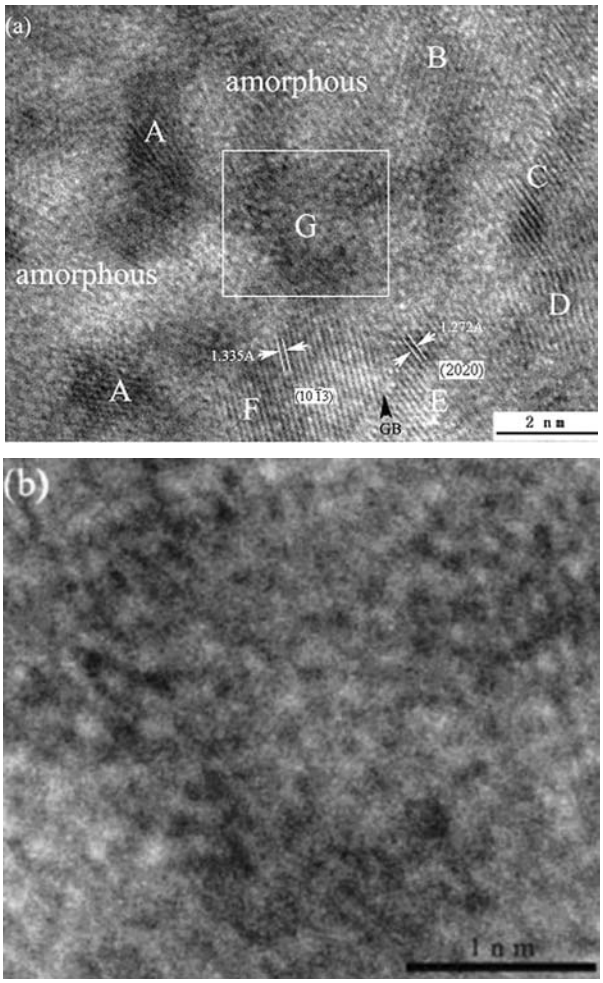

Figure 5 High-resolution crystal lattice image of selected area. (b) was the amplification of "G" area in (a).

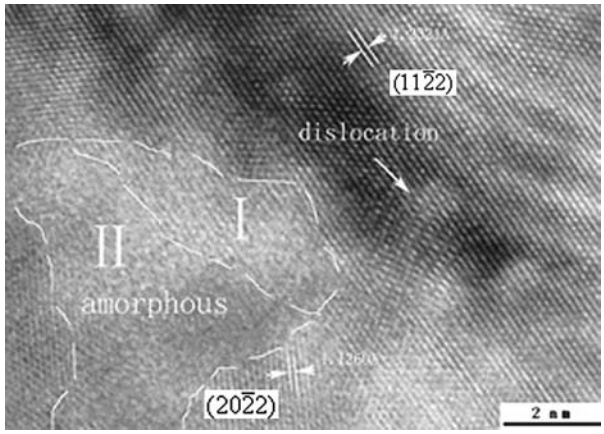

Figure 6 Coexistence of amorphous and nanograins in the Ti/Ti explosive bonding zone.

"B", "C", "D", "E", and "F" regions were range from 2 to 4 nm and the directions of fringes were different. So they were nanograins and the grain sizes were range from 2 to 4 nm.

Fig. 6 showed the coexistence of the amorphous and nanograins in the bonding zone. The up-right region was the lattice image of grain and the "II" area in the down-left region appeared as the characteristics of amorphous. Between them, the fringe patterns were ambiguous and the scales of the short-range ordered were still in certain degrees. Therefore, the "I" area was a transition area of amorphous and nanograins.

4. Discussion

Formation of amorphous and nanograins in the explosive bonding zone were usual considered as the result of the extreme rapid solidification. When the cooling rate of the melt was larger than 10^3 K/s, the number of crystal nucleus was increasing rapid and the grains were short of long-distance diffusion conditions before crystallizing, the homogeneous nanograins with or without obvious dendrite structure were formed. As long as the melt was super cooled to a certain degree, such as the amorphous transition temperature (Tg), the diffusion processes were terminated and then the amorphous were formed. How much was the cooling rate under the extreme conditions of the explosive cladding? Were there any other factors in favor of the formation of amorphous and nanograins during the explosive cladding?

4.1. Cooling rate

Formation of amorphous not only depended on a fast cooling rate at the beginning, but also required the cooling rate reaching a certain degree at the amorphous transition temperature (Tg) [10, 11]. Thus the study on the formation of amorphous in the bonding zone should build the temperature model of the bonding zone at first and then defined a Tg.

YAN and LI [11] had build the temperature model of the explosive bonding zone and pointed out that the distribution of temperature and cooling rate within the bonding zone could be expressed as follows:

$$T(0,t) = T_{\mathrm{m}}\sqrt{\frac{t_{\mathrm{r}}}{t}} \qquad (t > t_{\mathrm{r}}) \tag{1}$$

$$\frac{\partial T}{\partial t} = -\frac{T_{\mathrm{m}}}{2}\sqrt{t_{\mathrm{r}}}t^{-\frac{3}{2}} \qquad (t > t_{\mathrm{r}}) \tag{2}$$

where T_{m} was the melting point, t was time, and t_{r} was the time of tension wave back to explosive cladding interface which defined as follows:

$$t_{\mathrm{r}} = \frac{2H}{C_0} \tag{3}$$

where C_0 was the velocity of body wave and 2H was the thickness of plate.

In the present study, parameters of the flyer plate were: $H = 10$ mm, $T_{\mathrm{m}}= 1941$ K, $C_0 = 4695$ m/s. Substituted these data into equation (1) and (3), and the cooling rate was:

$$\frac{\partial T}{\partial t} = -2.003t^{-\frac{3}{2}} \tag{4}$$

When the time t was larger than 4.26 μs, the relation between time and the cooling rate in the bonding zone was showed in Fig. 7. With the increase of time, the cooling rate fast declined. At the beginning stage, the cooling rate reached approximately several 10^8 K/s, which was approach to the result (approximately 10^9 K/s) calculated by the cooling rule of the titanium plate [12].

In order to calculate the cooling rate at Tg, Tg should be estimated at first. Tg was a dynamic parameter determined by specific heat, coefficient of viscosity, and obvious change of specific heat within a narrow temperature interval in which the liquid metal was transformed into amorphous alloy. Because of the high melt point and strong activity and low possibility of formation amorphous, Tg of titanium alloy couldn't be easily determined. Nishiyama, *et al.* [13] prepared the titanium–based amorphous $Ti_{50}Cr_{10}Ni_{20}Cu_{20}$ by the two-stage quenching. Investigated by the differential scanning calorimetry, it showed that the cure of heat-release and temperature changed continuously and peaked at 630 K. That was to say, the titanium grains were precipitated from amorphous parent metal at the temperature closing to 630 K. Therefore, the Tg was less than 630 K. Generally, Tg of amorphous metals, such as Ni, $Fe_{91}B_9$, $Fe_{79}Si_{15}B_{11}$, Ge, Te and so on, were range from 0.25 to 0.62 T_{m} [1]. Thus Tg of titanium should be larger than 485 K (0.25 T_{m} of titanium). It was concluded that Tg of titanium was range from 485 k to 630 k.

Substituted equation (4) into equation (1), the relation between the cooling rate and temperature could be obtained, shown in Fig. 8. It could be seen that the cooling rates were 3.55×10^6 K/s and 7.80×10^6 K/s at the temperature 485 K and 630 K, respectively. They were larger than the usual requirement of cooling rate (10^5 K/s) of the formation of amorphous. Therefore, this condition was in favor of the formation of amorphous. In the bonding zone slightly away from the interface, the cooling rate was not enough to form the amorphous and then the nanograins were formed. So the coexisting of amorphous and nanograins was formed within the bonding zone.

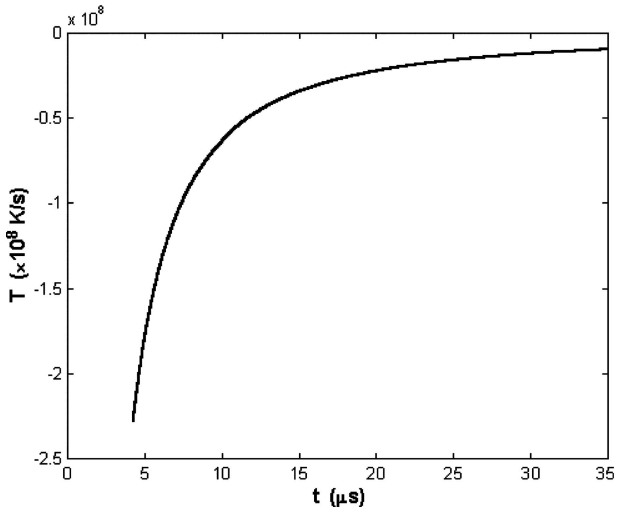

Figure 7 The cooling rate versus time curves obtained within the bonding zone.

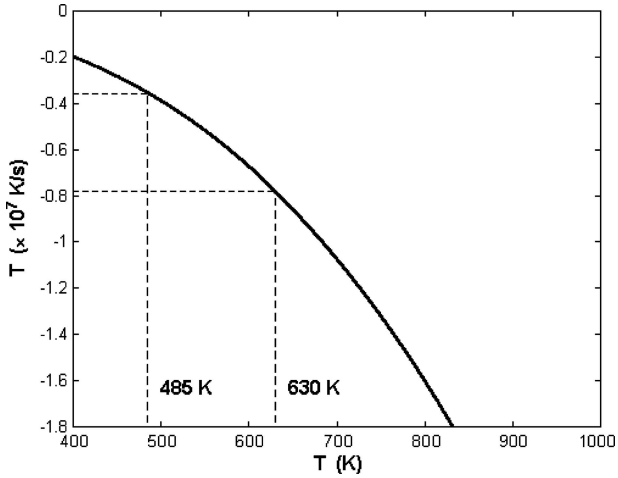

Figure 8 The cooling rate versus temperature curves obtained within the bonding zone.

4.2. Other factors

Yang [12] pointed out that the carbon atoms in the bonding zone were in favor of the formation of amorphous. Li and Liu [14] proposed that the monocrystalline gallium arsenide could generate nanocrystalline organization composed of nanograins and amorphous by the indentation method for the reason of combined action of high static pressure and shear stress. The lattices of the

monocrystalline gallium arsenide were distorted by the high pressure and shear stress and then formed the amorphous.

In the present study, the high pressure and high shear stress within the explosive bonding zone should be considered.

The flyer plate velocity was about 608 m/s and the impact pressure of explosive cladding corresponding to the velocity calculated by the impedance matching technique [15] was approximately 6.4 GPa. Under this high pressure, the grain density increased and the space of atom movement reduced and the long-range diffusion became difficult. These were not in favor of the formation of grain. Although the formation energy of steady-state phase was lower than the amorphous, the dynamic conditions of the formation of the steady-state phase were not enough under this pressure. So the super high pressure was favorable to form amorphous.

What's more, during the explosive cladding, the flyer plate collided with the base one at a certain angle and then the high shear stress generated in the interface. The crystal lattice was distorted by the high shear stress and led to local disorder. Added to the short duration of high temperature, the amorphous and nanograins were formed at last. It was concluded that the high pressure and shear stress within the bonding zone were favorable factors for the formation of amorphous and nano grains.

5. Conclusion

1. Nanograins and amorphous were formed in the Ti/Ti explosive bonding zone. Nanograins with perfect crystal structure were in coherent with the matrix and the grain sizes were range from 2 to 50 nm in diameter. Amorphous coexisted with nanograins were in the state of the long-range disorder.

2. High cooling rate in explosive bonding zone was the main reason for the formation of amorphous and nanograins. The amorphous transition temperature of titanium was varied from 485 to 630 K. Quantitative analysis indicated that the cooling rate reached approximately magnitude of 10^8 K/s at the beginning of the explosive cladding and that was range from 3.55 $\times$ 10^6 to 7.8 $\times$ 10^6 K/s at the amorphous transition temperature.

3. The pressure in the bonding zone was approximately 6.4 GPa during the explosive cladding. Crystal lattice was distorted by the high pressure as well as high shear stress and led to local disorder. Therefore they were also the favorable conditions of the formation of amorphous.

Acknowledgment

This work was supported by the Ph. D. Programs Foundation of Ministry of Education of China (No. 20020533015) and by National Nature Science Foundation of China (No. 50471059).

References

1. Y. H. WANG and Y. S. YANG, in "Amorphous metal" (Metallurgy Industry Press, Beijing, 1989) p. 2.
2. P. DUWEZ, R. H. WILLEUS and W. KLEMENT, *Applied Physical Letter.* **31** (1960) 1136.
3. H. S. CHEN, *Acta Metall.* **22** (1974) 1505.
4. J. J. HE, D. CHEN and Q. CHEN, *Hunan Metallurgy.* **5** (2002) 3.
5. D. J. LI, J. T. WANG and B. Z. DING, *Natural Science Process—communication of national major experimental laboratory.* **5** (1992) 562.
6. Y. YANG, X. M. ZHANG, Z. H. LI and Q. Y. LI, *Journal of central south industry mining metallurgy.* **10** (1994) 617.
7. Y. YANG, X. M. ZHANG and Z. H. LI, *Transactions of Nonferrous Metals Society of China.* **3** (1994) 93.
8. Y. YANG, X. M. ZHANG, Z. H. LI and Q. Y. LI, *Acta Mater.* **44** (1996) 561.
9. M. HAMMERSCHMIDT and H. KREYE, in Proceeding of an international conference on Metallurgical Effects of High-Strain-Rate Deformation and Fabrication, Albuquerque, June 1980, edited by M. A. Meyers and L. E. Murr (Plenum Press, New York, 1981) p. 961.
10. K. ZHANG and X. J. LI, *Journal de Physique III.* **1**(c) (1991) 229.
11. H. H. YAN and X. J. LI, *Rare Metal Materials and Engineering.* **32**(3) (2003) 176.
12. Y. YANG and X. M. ZHANG, *Chinese Journal of Materials Research.* **9**(2) (1995) 186.
13. N. NISHIYAMA, M. OGUCHI and A. INOUE *et al.*, *Materials Science and Engineering.* **A179–80** (1994) 697.
14. Z. C. LI and L. LIU *et al.*, *Chinese Journal of Materials Research.* **16**(2) (2002) 172.
15. P. S. DECARLI and M. A. MEYERS, in Proceeding of an international conference on Metallurgical Effects of High-Strain-Rate Deformation and Fabrication, Albuquerque, June 1980, edited by M. A. Meyers and L. E. Murr (Plenum Press, New York, 1981) p. 361.

Received 5 January
and accepted 22 July 2005